International Journal of Engineering Research And Development
e- ISSN: 2278-067X, p-ISSN: 2278-800X, www.ijerd.com
Volume 20, Issue 4 (April. 2024), PP. 41-48

Control of Permanent Magnet Synchronous Generator for Wind Power Systems

[1]C. A. Obiora-Okeke, [1]D. C. Oyiogu, [1]U. E. Anionovo, [1]H. N. Ogboke, [1]K. C. Obute, [2]C. J. Ofuase
[1]*Department of Electrical Engineering, Nnamdi Azikiwe University, Awka, Nigeria*
[2]*Department of Electrical/Electronic Engineering, University of Benin, Edo State, Nigeria*

ABSTRACT
This work presents the control of 315kW Permanent Magnet Synchronous Generator (PMSG) wind power system, which has a full-scale Voltage Source Converter (VSC) for generator side control. Mathematical models of the VSC and PMSG were developed in the direct-quadrature (dq) synchronous reference frame, in order to implement stator field oriented control (FOC). Matlab/Simulink was used to model the wind power system and tune the proportional and integral (PI) controllers. The simulation results show that the PI controllers of current and speed loops produce very good performance.

Date of Submission: 04-04-2024 Date of Acceptance: 15-04-2024

I. INTRODUCTION

Rise in the demand for environmentally friendly electrical power sources has increased the growth of wind power systems due to concerns regarding pollution from fossil fuel and nuclear energy electrical power sources, as well as, high and fluctuating price of crude oil. According to [1], the current global wind generation and installed wind energy capacity are $2.1x10^6$GWh and 898.82GW respectively. With China leading with an installed capacity of 327GW [2], it is predicted that global installed wind energy capacity will reach 2,000GW by 2030, and thereby supply 17-19% of the world's electricity [3].

In addition, advances in semiconductor compounds such as Silicon Carbide (SiC) and Gallium Nitride (GaN) have brought about improvements in power electronic components leading to reliable and cost effective deployment of full scale power converters in variable speed direct drive wind power systems [4].

The topology of the wind power system in this work consists of a 315kW variable speed wind turbine with surface mounted Permanent Magnet Synchronous Generator (PMSG) and a full-scale voltage source converter (VSC), which comprises a back-to-back VSC and a DC link capacitor that allows bidirectional power flow between the grid side VSC and generator side VSC. The configuration presented requires the following control techniques: pitch angle control, which is used to prevent the wind turbine's output power from exceeding the rated value; the generator side VSC control used to regulate the generator rotor speed, a constant DC link control, as well as, the grid side VSC control, which is used for active and reactive power control. The focus in this work is a generator side control scheme implemented with stator field oriented control and sinusoidal pulse width modulation.

II. THE WIND POWER SYSTEM MODEL

In this section, the description of the wind turbine system and mathematical models of PMSG and VSC are presented. Fig. 1 below shows the configuration of a direct drive full scale PMSG connected to the grid through a back-to-back VSC.

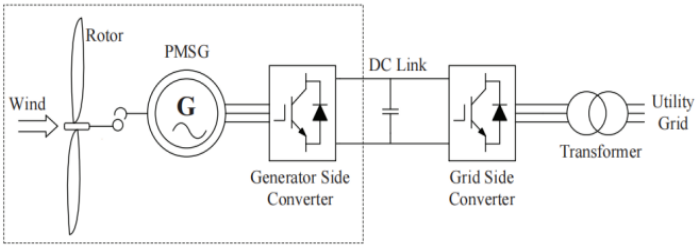

Fig. 1: Variable Speed PMSG Wind Power System with back-to-back VSC

A. Wind Turbine System Description

The 3 main components of a horizontal wind turbine are: the tower, which supports the turbine, ensures it is clear from the ground and allows it to reach stronger winds; the nacelle, which houses the shaft and the generator; and the turbine rotor, which extracts power from the wind. The power obtained from a wind turbine is a function of air density ρ, area swept by the turbine rotor blade of radius R, wind speed V_w and coefficient of power C_P. The extracted power is governed by (1) below [5].

$$P = 0.5\rho\pi R^2 V_w^3 C_p \quad (1)$$

In practice, 100% energy cannot be extracted from wind, because the flow of air over the turbine blades makes it spin, as a result the turbine blades slow down the wind to extract energy. Consequently, the theoretical limit to which the turbine blades can extract energy is 59.26% referred to as the Betz Coefficient. Due to the aerodynamics of the turbine rotor, the coefficient of power C_p is less than the Betz Coefficient.

Subsequently, the coefficient of power depends on two other parameters, the tip speed ratio λ, and the pitch angle β. The tip speed ratio is the ratio of the product of the radius R, and the angular speed of the turbine blade w_r to the wind speed [5], [6]. Also, the mechanical torque T_m is the ratio of power P to turbine angular speed as expressed in (2) below.

$$T_m = \frac{0.5\rho\pi R^2 V_w^3 C_p}{w_r} \quad (2)$$

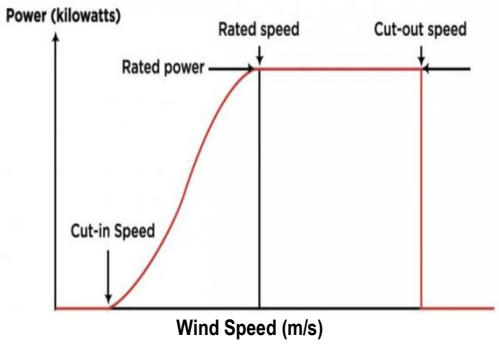

Fig. 2: Wind Power Curve

The relationship between the output power, wind speed and control of the wind turbine is presented in the power curve of Fig. 2 above. It depicts three operating conditions namely: cut-in speed, usually 4m/s, which is the wind speed when rotation and power generation occurs; rated speed, between 11-17m/s, which is the wind speed at which the turbine output power equals the electrical power limit of the generator, and cut-out speed, the wind speed at which pitch control is used to stop the rotation of the turbine blade, in order to prevent damage to the turbine blades and structure, typical 25m/s.

B. Modelling of PMSG

In [7], [8] signals in the direct-quadrature (dq) synchronous reference frame are D.C waveforms, which brings about easy analysis and control design. Therefore, this reference frame was used to develop the model of PMSG as expressed by the flux, voltage and torque equations respectively in (3), (4) and (8) below [4].

Additionally, λ_{sd}, λ_{sq}, i_{sd}, i_{sq}, v_{sd}, v_{sq}, L_{sd} and L_{sq} are the d-axis stator flux, q-axis stator flux, d-axis stator current, q-axis stator current, d-axis stator voltage, q-axis stator voltage, d-axis stator inductance and q-axis stator inductance respectively.

$$\begin{bmatrix}\lambda_{sd}\\ \lambda_{sq}\end{bmatrix} = \begin{bmatrix}L_d & 0\\ 0 & L_q\end{bmatrix}\begin{bmatrix}i_{sd}\\ i_{sq}\end{bmatrix} + \begin{bmatrix}\lambda_m\\ 0\end{bmatrix} \quad (3)$$

$$\frac{d}{dt}\begin{bmatrix}\lambda_{sd}\\ \lambda_{sq}\end{bmatrix} = \begin{bmatrix}0 & w_e\\ -w_e & 0\end{bmatrix}\begin{bmatrix}\lambda_{sd}\\ \lambda_{sq}\end{bmatrix} + \begin{bmatrix}-R_s & 0\\ 0 & -R_s\end{bmatrix}\begin{bmatrix}i_{sd}\\ i_{sq}\end{bmatrix} + \begin{bmatrix}v_{sd}\\ v_{sq}\end{bmatrix} \quad (4)$$

solving (3) and (4) yields (5) below.

$$\frac{d}{dt}\begin{bmatrix}\lambda_{sd}\\ \lambda_{sq}\end{bmatrix} = \begin{bmatrix}0 & w_e\\ -w_e & 0\end{bmatrix}\begin{bmatrix}\lambda_{sd}\\ \lambda_{sq}\end{bmatrix} + \begin{bmatrix}-R_s & 0\\ 0 & -R_s\end{bmatrix}\begin{bmatrix}i_{sd}\\ i_{sq}\end{bmatrix} + \begin{bmatrix}0\\ -w_e\lambda_m\end{bmatrix} + \begin{bmatrix}v_{sd}\\ v_{sq}\end{bmatrix} \quad (5)$$

eliminating λ_{sd} and λ_{sq} from (5) gives (6) below

$$\frac{d}{dt}\begin{bmatrix} L_d i_{sd} \\ L_q i_{sq} \end{bmatrix} = \begin{bmatrix} 0 & L_q w_e \\ -L_d w_e & 0 \end{bmatrix}\begin{bmatrix} i_{sd} \\ i_{sq} \end{bmatrix} + \begin{bmatrix} -R_s & 0 \\ 0 & -R_s \end{bmatrix}\begin{bmatrix} i_{sd} \\ i_{sq} \end{bmatrix} + \begin{bmatrix} 0 \\ -w_e \lambda_m \end{bmatrix} + \begin{bmatrix} v_{sd} \\ v_{sq} \end{bmatrix} \quad (6)$$

$$T_e = \frac{3}{2} n_p [\lambda_m i_{sq} + [L_d - L_q] i_{sd} i_{sq}] \quad (7)$$

Also, R_s represents stator resistance, T_e is the electromagnetic torque, n_P stands for number of pole pairs, w_e is the electrical angular speed of the generator rotor, and λ_m denotes the maximum flux generated by the rotor magnets. Since a round nonsalient rotor is employed, $L_d = L_q$. Therefore, (7) results in (8) below.

$$T_e = \frac{3}{2} n_p \lambda_m i_{sq} \quad (8)$$

The dynamic torque characteristics of the wind turbine is given in (9), where J is moment of inertia, F is viscous friction coefficient and T_m is mechanical torque.

$$T_e = J\frac{dw_r}{dt} + T_m + F w_r \quad (9)$$

C. Modelling of the VSC

From Fig. 1 above, the generator-side VSC controls generator's rotor speed and torque, and serves as a rectifier. Its circuit is represented in Fig. 3 below. Reference [9] derived the three-phase mathematical model of the VSC presented in (10) to (12) under the assumption of a balanced three-phase system, without neutral connection and negligible resistance of the VSC.

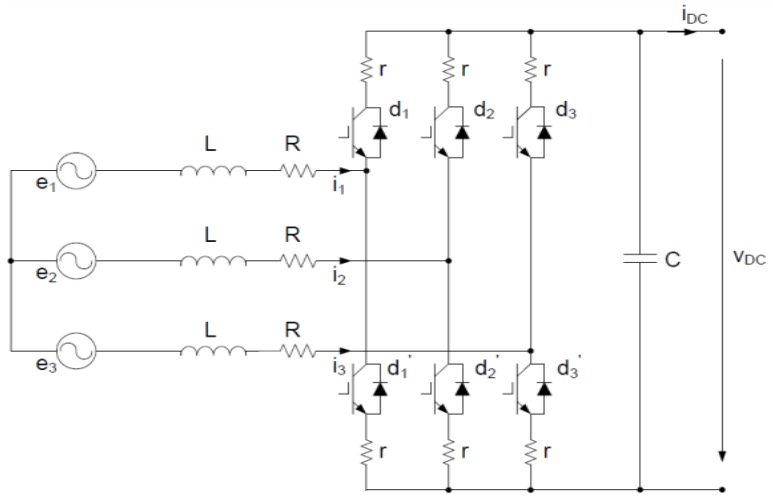

Fig. 3: Circuit Diagram of a Three-phase VSC

$$C\frac{dV_{dc}}{dt} = \sum_{k=1}^{3} i_k \, d_k - i_{dc} \quad (10)$$

$$L\frac{di_k}{dt} + Ri_k = e_k - V_{dc}\left(d_k - \frac{1}{3}\sum_{n=1}^{3} d_n\right) \quad (11)$$

$$\sum_{k=0}^{n} e_k = \sum_{k=1}^{3} i_k = 0 \quad (12)$$

where

k	index for the three-phases = {1, 2, 3};
d_k	switching functions;
i_k	line currents;
e_k	phase voltage;
V_{dc}	bus voltage;

i_{dc} bus current;
R resistance of the stator;
L inductance of the stator;

applying Clarke and Park Transformations to
(10) to (12) gives (13) to (15) below.

$$C\frac{dV_{dc}}{dt} = \frac{3}{2}\left(i_q d_q + i_d d_d\right) - i_{dc} \quad (13)$$

$$L\frac{di_q}{dt} + Ri_q + w_e Li_d = e_q - V_{dc}d_q \quad (14)$$

$$L\frac{di_d}{dt} + Ri_d - w_e Li_q = e_d - V_{dc}d_d \quad (15)$$

applying Laplace transforms to (13) to (15) assuming zero initial condition, yields (16) to (18) below.

$$SCV_{dc} = \frac{3}{2}\left(i_q d_q + i_d d_d\right) - i_{dc} \quad (16)$$

$$SLi_q + Ri_q + w_e Li_d = e_q - V_{dc}d_q \quad (17)$$

$$SLi_d + Ri_d - w_e Li_q = e_d - V_{dc}d_d \quad (18)$$

Using equations (16) to (18), the block diagram of the VSC in the dq synchronous reference frame is derived and represented in Fig. 4 below.

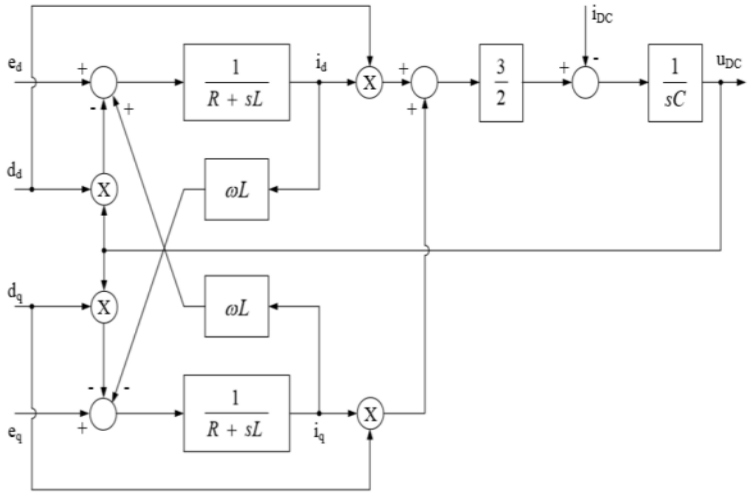

Fig. 4: A Model of the Three-Phase VSC in the dq Synchronous Reference Frame

Furthermore, in sinusoidal pulse width modulation (SPWM), the three-phase reference signals for the half bridges of the three-phase VSC are compared against the carrier signal, in order to generate the PWM turn ON/OFF commands for the VSC [10]. The switching function:

$$d_k = \begin{cases} 1, & ON \quad STATE \\ 0, & OFF \ STATE \end{cases} \quad (19)$$

determines the duty cycle. Also, $V_t = \frac{MV_{DC}}{2}$ subject to $0 \leq M \leq 1$ [7]. Where M, which represents the modulation index is the ratio of the reference signal to the carrier signal.

III. CONTROL OF PMSG

Stator field oriented control (FOC), a class of vector control, brings about the control of dynamic states of the PMSG, as well as, the position of the stator current vector. The goal of stator FOC is the spatial control of the orientation of the stator current vector of the PMSG [11]. As shown in Fig. 5, Clarke and Park transformations are employed in transforming the PM motor relations stated in (5) using the integral of the electrical angular speed obtained from the resolver or encoder's speed measurement.

Furthermore, the PM flux is anchored on the direct axis of the rotor and the feedback control schemes comprise an outer speed control loop and two inner current control loops, which are required to be faster than the outer speed control loop. With respect to [7], [11], in the current control loop, the d-axis reference current I_{sdref} is

set to zero to maximize torque and to reduce ohmic losses and the q-axis reference current I_{sqref} is acquired from the output of the speed PI controller. Also, the torque producing current I_{sq}, and the current of the d-axis I_{sd}, which contributes to the main flux are compared with their reference values to yield corresponding error signals. Consequently, the PI controllers process the error signals to produce the dq-axis voltages.

In addition, the decoupled voltages undergo inverse Park and Clarke transformations and are combined with the D.C voltage V_{DC} to create modulating signals for PWM.

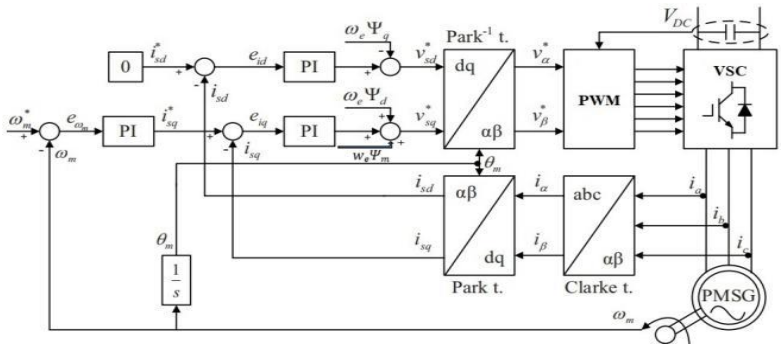

Fig. 5: Block Diagram of FOC

A. Current Control Loop

Supposing u_d and u_q are as expressed in (20) and (21),

$$u_d = L_q w_e i_{sq} + V_{sd} \tag{20}$$

$$u_q = -L_d w_e i_{sd} - \lambda_m w_e + V_{sq} \tag{21}$$

(6) can be expressed as,

$$\frac{L_d di_{sd}}{dt} + R_s i_{sd} = u_d \tag{22}$$

$$\frac{L_q di_{sq}}{dt} + R_s i_{sq} = u_q \tag{23}$$

Adding the decoupling terms $-i_{sq} L_q w_e$ to the output of the d-axis PI current controller, as well as, $i_{sd} L_d w_e$ and $\lambda_m w_e$ to the output of the q-axis PI current controller, two independent closed loop control subsystems of the stator are developed as shown in figure 6 below. The Kp and Ki values were obtained by tuning the PI controllers of control system tool box in Matlab/Simulink.

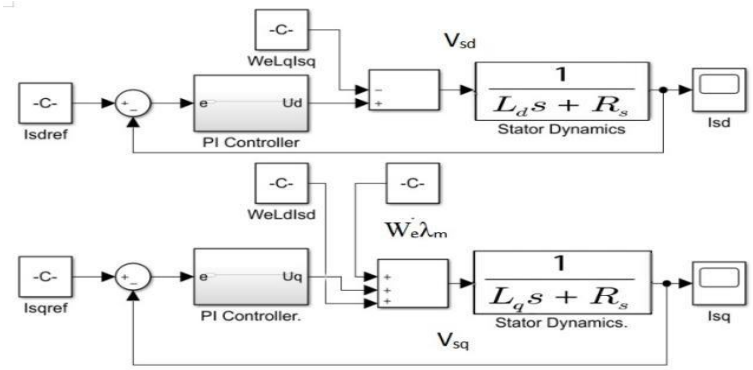

Fig. 6: d and q axis Current Control Loop

B. Speed Control Loop

The rotor speed, which is obtained from an estimator or measurement with an encoder increases as the wind speed increases. When the rotor speed reaches its rated speed of 6.221rad/s, and the wind speed continues

to increase beyond its rated value of 11.5m/s, the PI controller ensures that the rated rotor speed is maintained as the wind speed fluctuates above its rated value. Similar to the current controller, Kp and Ki values were obtained by tuning the PI controller of the control system tool box in Matlab/Simulink.

Table 1. Wind Turbine Parameters

Parameter	Value
Rated Power	315kW
Blade Radius (m)	15
Rated Speed (rpm)	59.4
Rated Torque (Nm)	50,643
Minimum Wind speed (m/s)	4
Maximum Wind Speed (m/s)	25
Shaft Stiffness Coefficient (K_{lss}) (Nm)	43,532,665
Shaft Damping Coefficient (D_{lss}) (Nm/s)	1,519,465
Inertia (Kg/m2)	90,632

Table 2. Generator Parameters

Parameter	Value
Rated Mechanical Power (kW)	315
Rated Stator line-line voltage (V)	415
Pole Number	96
Stator Resistance (Ohms)	0.0054
Stator Inductance (mH)	0.9
Mutual Inductance (mH)	0.54
Stator Flux (Wb)	1.3
Inertia (Kg/m2)	50

IV. SIMULATION RESULTS

A. Current Loop Response

From Fig. 7 below, the PI controller's gain values, Kp = 200 and K_i = 2000, maintain the d-axis rotor reference frame measured current I_{sd} at zero, with negligible deviation from the reference value during the transient condition. Also, for PI controller's gain values K_p = 200 and K_i = 2000, the q-axis rotor reference frame measured current I_{sq} tracks its reference I_{sqref} with minimal overshoot as shown in Fig. 7.

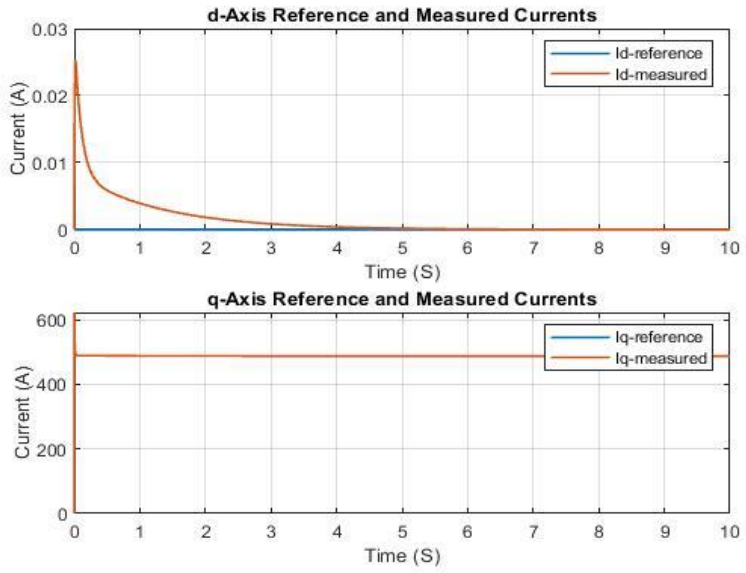

Fig. 7: dq-Axis Reference and Measured Currents

B. Speed Loop Response

At the rated wind speed of 11.5m/s, the PI controller's gain values K_p = 100 and K_i = 500 ensure the measured rotor speed of the PMSG tracks the reference speed without oscillations and overshoot as shown in Fig. 8. It can be observed from the slow transient response that due to the high inertia of the wind power system; it requires considerable time to achieve steady state.

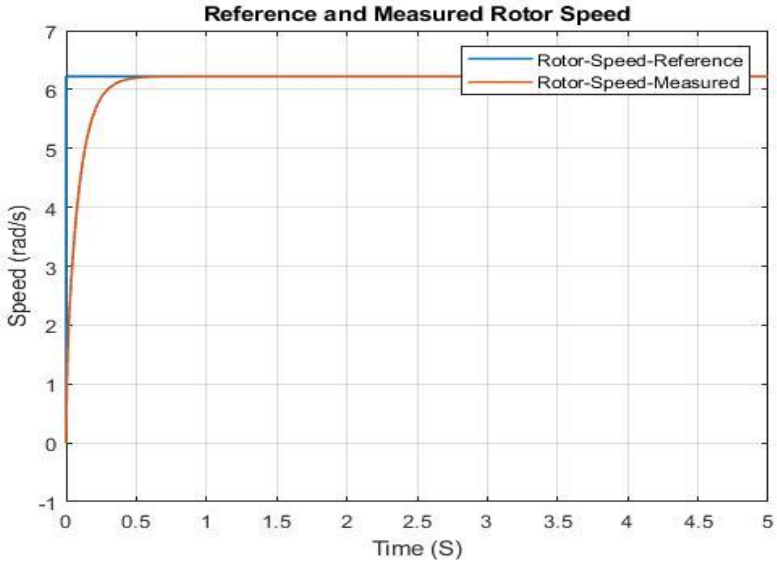

Fig. 8: Reference and Measured Rotor Speed

V. CONCLUSION

This work focuses on the control of 315kW PMSG wind power system, where only the generator VSC control was addressed. The mathematical models of the VSC and PMSG were presented and stator FOC scheme was implemented to control the dq-axis currents and rotor speed. In respect of future work, implementation of Direct Torque Control is recommended for comparison with stator FOC.

REFERENCES

[1] International Renewable Energy Agency. (2023) https://ourworldindata.org/grapher/cumulative-installed-wind-energy-capacity-gigawatts [online]. Available

[2] https://www.evwind.es/2023/01/14/countries-produced-the-most-wind-energy.[online]. Available

[3] https://gwec.net/globalwindreport2023 [online]. Available

[4] F. Blaabjerg, F. Iov, Z. Chen, K. Ma, "Power Electronics and Controls for Wind Power Systems," IEEE Intl. Energy Conf., Manama Bahrain, Dec. 18-22, 2010.

[5] Y. Errami, M. Oussaid, M. Maaroufi, "Control of a PMSG Based Wind Energy Generation System for Power Maximization And Grid Fault Conditions," Energy Procedia Science Direct Elsevier Ltd., vol. 42, pp. 220-229, Nov. 2013, doi:10.1016/j.egypro .2013.11.022.

[6] J.A. Baroudi, V. Dinavahi, A.M. Knight. "A Review of Power Converter Topologies for Wind Generators,"Renewable Energy Science Direct Elsevier Ltd., vol. 32, no. 14, pp. 2369-2385, Jan. 2007, doi:10.1016/j.renene.2006.12.002

[7] A. Yazdani, R. Iravani, Voltaged-Sourced Converters in Power Systems: Modelling, Control and Applications. Hoboken, New Jersey, USA: John Wiley & Sons, Inc.,2010.

[8] S. B. Shahapure, V. A. Kulkarni Deodhar, "Modeling and Field Oriented Control of Permanent Magnet Synchronous Motor Drive," IEEE 8th Intl. Conf. for Convergence in Tech. (I2CT), Lonavla, India, 2023, pp. 1-5, doi: 10.1109/I2CT57861.2023.10126498.

[9] V. Blasko, V. Kaura, "A New Mathematical Model and Control of a Three-Phase AC–DC Voltage Source Converter." IEEE Trans. on Power Electronics. vol. 12, no. 1, pp. 116-123, Jan. 1997

[10] B. Sakthisudhursun, S. Muralidharan, "Low Cost Microcontroller based Experimental Setup to Study Sinusoidal Pulse Width Modulation for Multilevel Inverter," Intl. Conf. on Power, Instrum., Energy and Control (PIECON), Aligarh, India, 2023, pp.1-6, doi: 10.1109/PIECON56912.2023.10085863.

[11] C. Busca, A. -I. Stan, T. Stanciu and D. I. Stroe, "Control of Permanent Magnet Synchronous Generator for large wind turbines," IEEE Intl. Symp. on Industrial Electronics, Bari, Italy, 2010, pp. 3871-3876, doi:10.1109/ISIE.2010. 5637628.